Experimental Identification and Control of a 3Kw DC Motor

Mohamed Lamine Hamida[1]*, Arezki Fekik[1,2], Hakim Denoun[1], Farid Kadi[1]

[1] Electrical Engineering Advanced Technology Laboratory (LATAGE), Departement of Electrical Engineering, Mouloud Mammeri University, 15000 Tizi Ouzou, Nouvelle ville, P.O.B. 15000, Algeria
[2] Departement of Electrical Engineering, Akli Mohand Oulhadj University, 10000 Bouira, Drissi Yahia, P.O.B. 10000, Algeria
* Corresponding author, e-mail: mohamedlamine.hamida@ummto.dz

Abstract

In this project, it was requested to identify the parameters of a 3Kw DC machine to realize a speed control of this machine using a Dspace1103 acquisition card. The control consists to generate a PWM signal to manage a buck chopper based on an IGBT. The proposed control is based on two Proportional-Integral (PI) controllers to regulate both, the speed and the current of the identified DC motor. For this purpose, tests were carried out in order to identify the parameters of this machine. This was followed by the practical implementation of our control system. In order to validate our test bench, several diagrams and explanations have been presented in this paper. The proposed algorithm has been investigated through simulation using the MATLAB/Simulink environment and validated experimentally on a laboratory prototype using Dspace1103 real time board.

Keywords

DC motor, identification, PI controller, Dspace1103

1 Introduction

Drives using the DC machine occupy an important place in the industrial sector, such as handling, grinding, where it is necessary to control the speed [1–4].

The connection of a direct current motor to the same type of source is done by means of a static converter, which allows the variation of the average voltage at the terminals of the armature. Until recent years, the control of industrial static converters was carried out using analog circuits with low or medium degree of integration [5, 6].

To build controllers and meet performance goals, it is necessary to understand the system's dynamic model. It is not necessary to find a precise mathematical model for control purposes, but it is necessary to have a model that considers the major dynamics [7].

One of the great problems in controlling of DC motors is the lack of information regarding the parameters that constitute the mathematical model. Often the motor is worn out due to its use, which makes its information out of date. Thus, a model with imprecise parameters can reduce the efficiency of the control system [8, 9].

The load torque and network voltage might induce destabilization of the actual speed and current during the operation of the DC motor, which is undesirable. As

a result, controlling the DC motor's speed and current is critical [10]. The regulation operates on two fronts:

1. the DC motor's speed, and
2. the armature current, keeping it within acceptable limits in scenarios like quick start, sudden change in resistive torque, sudden braking, or very rapid increase in the speed set point.

The structure of a speed controller for a DC motor usually consists of two loops.

The first loop compares the current speed to the reference speed, while the second loop regulates the armature current. The objective of our work is to identify the parameters of a DC machine, then to design a speed control of this machine via a DC-DC buck converter.

To ensure this control, we have opted for a PI controller. The Proportional-Integral (PI) controller is often used to control electric actuators [11–13]. The main characteristics of the PI controller are its simplicity and its ability to maintain a zero steady state error when the reference is changed [14, 15]. The proposed algorithm is implemented on Dspace1103 with MATLAB/SIMULINK software.

The work that we have done is articulated around three points. The first, is devoted to the modeling and identification of the parameters of the DC machine. The second part is dedicated to the calculation of the motor's speed and the current regulators. In Section 3, we present the experimental device and the obtained results.

2 Modeling of a DC motor

The separately excited DC motor has two windings, each one powered by a separate power supply voltage [16, 17]; Fig. 1 shows the equivalent circuit of separately excited motor; where R_a and L_a represent respectively the resistance and the inductance of the armature winding. The resistance and the inductance of the field winding are presented by R_f and L_f, E_a is the emf induced in the armature circuit, ω_r the motor speed, k_b is the back emf constant, T_e and T_L respectively the motor and the load torque, K_f is the viscous friction coefficient and J the total inertia of motor .

The mathematical model of the DC motor consists of electrical and mechanical equations, these two groups of equations allow us to understand better the DC motor in its real operation [18]. This model is determined by Eqs. (1) to (4):

$$V_a(t) = R_a I_a(t) + L_a \frac{dI_a(t)}{dt} + E_a(t), \tag{1}$$

$$V_f(t) = R_f I_f(t) + L_f \frac{dI_f(t)}{dt}, \tag{2}$$

$$E_a(t) = k_b \omega_r(t), \tag{3}$$

$$T_e = J \frac{d\omega(t)}{dt} + K_f \omega_r(t) + T_L. \tag{4}$$

The parameters mentioned on the nameplate of the machine available in the laboratory are listed in Table 1.

3 Identifying the parameters of a DC motor

The identification of the parameters of the DC machine consists in carrying out tests on it. The parameters to be
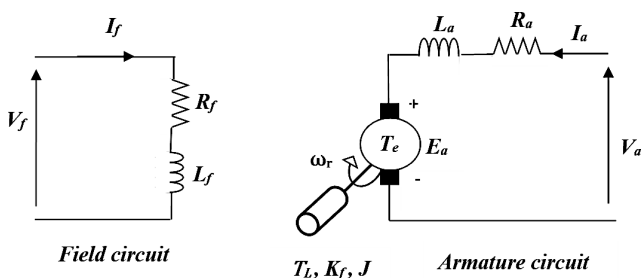
Fig. 1 Separately excited DC motor

Table 1 Nameplate parameters

Nominal armature voltage	220 V
Tension field voltage	110 V
Nominal armature current	16 A
Nominal field current	1.32 A
Power	3 Kw
Nominal torque	19 Nm
Nominal motor speed	1500 rpm

identified are; the armature resistance R_a, the armature inductance L_a and those of the inductor R_f and L_f, the constant of the back electromotive force K_e, the coefficient of friction K_f, and the moment of inertia J [19].

There are several methods of identifying the parameters of the DC machines. We will proceed in this work to the determination of these parameters via a practical and a simple method.

3.1 Measurement of the R_a and R_f resistances

The armature and the inductor resistances are measured in the hot state by the volt-amperometric method, the measurements are carried out at different values of the intensity (up to 30% of the nominal current to avoid overheating of the machine) [20].

3.2 Measurement of the L_a and L_f inductances

The AC supply of the armature with an open inductor and vice versa directly gives the inductances of each winding.

$$L_a = \frac{1}{2\pi f} \sqrt{\left(\frac{V_a}{I_a}\right)^2 - R_a^2} \tag{5}$$

$$L_f = \frac{1}{2\pi f} \sqrt{\left(\frac{V_f}{I_f}\right)^2 - R_f^2} \tag{6}$$

3.3 Determination of the EMF constant of the DC motor

It suffices to carry out an off-load test and note the characteristic $V_a(I_f)$, the motor must operate as a generator and must be driven at its nominal speed, the slope of this characteristic represents the quantity $M_{fd} \cdot \omega_r$. It is then sufficient to divide this slope by the speed of rotation expressed in rd/s, since the no-load armature voltage is expressed by the relation (Eq. (7)):

$$V_a = M_{fd} \cdot \omega_r \cdot I_f, \tag{7}$$

and the constant of the back electromotive force K_e is given by:

$$K_e = M_{fd} \cdot I_f. \tag{8}$$

3.4 Determination of mechanical parameters

The fundamental differential equation of mechanics governing the dynamic operation of an electrical machine is expressed by:

$$J \frac{d\omega_r}{dt} = C_m - C_s - K_f \omega_r. \tag{9}$$

3.4.1 Determination of dry friction torque and viscous friction coefficient

At off-load, the electromagnetic torque is written:

$$C_{em} = C_s + K_f \omega_r. \tag{10}$$

Knowing that the electromagnetic torque is proportional to the current of the armature:

$$C_{em} = K_e \cdot I_a, \tag{11}$$

we will get:

$$K_e \cdot I_a = K_f \omega_r + C_s. \tag{12}$$

To plot $K_e \cdot I_a = f(\omega_r)$, the no-load motor is supplied with variable voltage in order to vary I_a and ω_r, the plot gives a straight line of the form $y = ax + b$ as shown in Fig. 2.

At the intersection of the ordinate axis, the value of C_s is read. The coefficient of friction K_f is the slope of this characteristic.

3.4.2 Identification of the moment of inertia

After starting the DC motor, the voltage is set to its nominal value. The power supply to the armature is cut off, the inductor remains supplied separately.

At $t = 0$, the following quantities are noted: $V_o = V_n$, I_o, ω_{ro}, and the time taken by the motor to stop is also recorded.
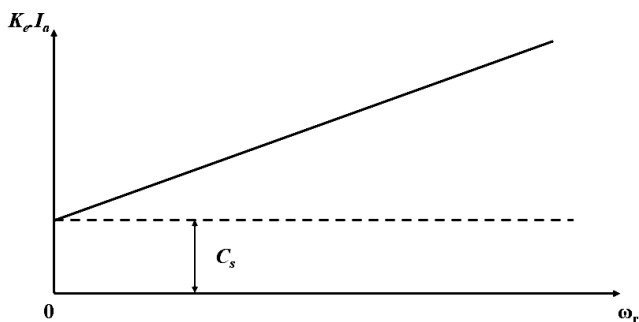
Fig. 2 Characteristic of the electromagnetic torque

Disregarding the signs, in the case of no-load we can write:

$$J \frac{d\omega_r}{dt} = C, \tag{13}$$

$$J = \frac{\int_0^T dt}{\int_0^{\omega_r} \frac{d\omega_r}{C}}. \tag{14}$$

Since C is a function of ω_r, the power taken from the network is:

$$P_{ab} = V_n \cdot I_0 = P_0 + R_a I_0^2. \tag{15}$$

Hence:

$$P_0 = I_0 (V_n - R_a I_0). \tag{16}$$

On the other hand:

$$P_0 = C \omega_r, \tag{17}$$

we deduce:

$$C = \frac{I_0 (V_n - R_a I_0)}{\omega_r}, \tag{18}$$

then:

$$J = \frac{T}{\int_0^{\omega_r} \frac{\omega_r d\omega_r}{P_0}}. \tag{19}$$

It is therefore interesting to plot the characteristic $\omega_r / P_0 = f(\omega_r)$. The different speeds will be obtained by varying the supply voltage, hence the variation of P_0. It is also fundamental to keep the excitation at its constant value.

The denominator of the expression for J in relation (Eq. (18)) represents the area between the axes, the curve $\omega_r / P_0 = f(\omega_r)$ and the ordinate at point ω_{ro} [21].

4 Practical tests

4.1 Determination of the R_a and R_f resistances

In order to determine the armature resistance, we use the volt-amperometric method. For this, we measure the armature current and voltage, without the excitation of the machine, and vice versa for the measurement of the inductor resistance as shown in Figs. 3 and 4.

The obtained results are shown in Tables 2 and 3. We can therefore determine the armature resistance using Ohm's law.

The average resistance values are:

$$R_a = 1.35 \ \Omega; \ R_f = 65.15 \ \Omega.$$
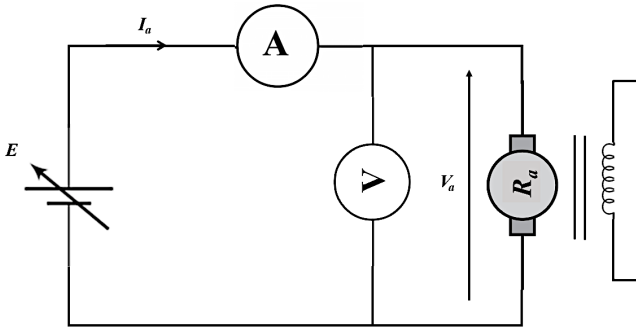
Fig. 3 Determination of the armature resistance R_a
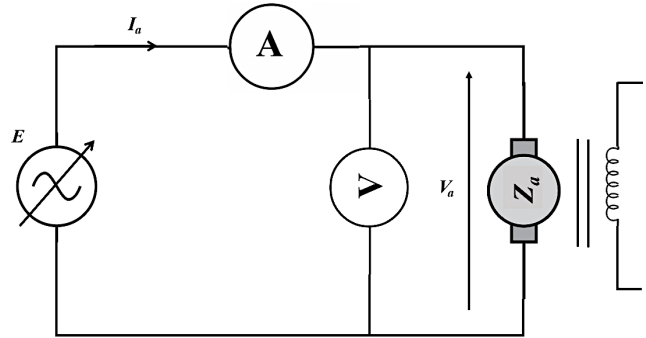
Fig. 5 Determination of the armature inductance L_a
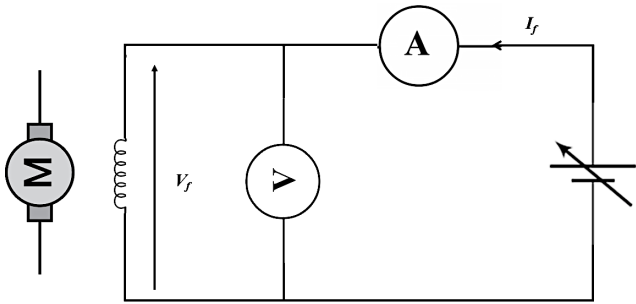
Fig. 4 Determination of the inductor resistance R_f
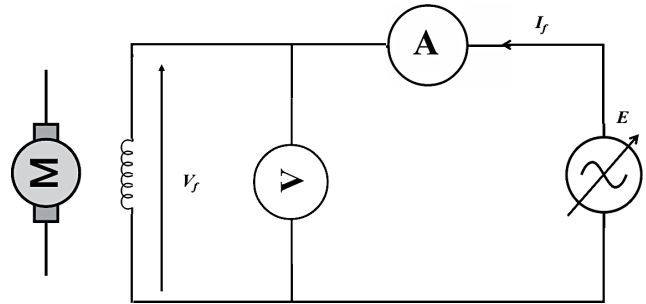
Fig. 6 Determination of the inductance of the inductor L_f

Table 2 Results obtained for the calculation of R_a

Measured V_a (V)	4.4	7	9.1
Measured I_a (A)	3.1	5.2	6.9
Calculated R_a (Ω)	1.42	1.35	1.32

Table 3 Results obtained for the calculation of R_f

Measured V_f (V)	32	51.8	66.7
Measured I_f (A)	0.5	0.8	1
Calculated R_f (Ω)	64	64.75	66.7

Table 4 Results obtained for the calculation of L_a

Measured V_a (V)	4.3	6.7	8.7
Measured I_a (A)	1.8	2.9	3.9
Calculated Z_a (Ω)	2.38	2.31	2.23

Table 5 Results obtained for the calculation of L_f

Measured V_f (V)	91	100	122
Measured I_f (A)	0.035	0.038	0.046
Calculated Z_f (Ω)	2600	2631.5	2652.2

4.2 Determination of the L_a and L_f inductances

We supply the armature of the motor with an alternating voltage V_a. For different values of V_a and I_a, we deduce the value of the inductance through the calculation of the average impedance Z_a of the armature. The proposed setup shown in Figs. 5 and 6. The obtained results are shown in Tables 4 and 5.

The average value of the impedances gives us:

$$Z_a = 2.3 \ \Omega; \ Z_f = 2627.9 \ \Omega.$$

For the calculation of the inductance, we follow these steps. The expression of the impedance is given by:

$$Z_a = \frac{V_a}{I_a} \ \text{and} \ Z_a = \sqrt{\left(R_a^2 + \left(L_a \omega\right)\right)^2},$$

with: $\omega = 2\pi f$; $f = 50$ Hz.

And finally, we deduce the inductance:

$$L_a = \frac{1}{2\pi f} \sqrt{\left(Z_a^2 - R_a^2\right)}.$$

After the calculations we find:

$$L_a = 0.0059 \ \text{H}; \ L_f = 8.35 \ \text{H}.$$

Now that we have the value of the resistance and the inductance, we can deduce the electrical time constant as follows:

$$T_e = L_a / R_a = 0.0059 / 1.35 = 0.0043 \ \text{s}.$$

4.3 Determination of the EMF constant of the DC motor

It suffices to perform an off-load test and note the characteristic $V_a \cdot (I_f)$, the motor must operate as a generator and must be driven at its rated speed. The slope of this

characteristic represents the quantity $M_{fd} \cdot \omega_r$. It then suffices to divide this slope by the speed of rotation expressed in rd/s, since the no-load armature voltage is expressed by the relation $V_a = M_{fd} \cdot \omega_r \cdot I_f$, and the constant K_e is given by: $K_e = M_{fd} \cdot I_f$. The proposed assembly is in Fig. 7. The obtained results are represented in Table 6. The rotor is driven at a speed of 1488 rpm.

The slope of the curve $V_a(I_f)$ gives us the value of $M_{fd} \cdot \omega_r$; to find the value of M_{fd} just divide this value by ω_r (Fig. 8), the obtained value is 1.07 H.

The excitation current is fixed at the nominal value, the value of the constant K_e can be deduced by the following relationship:

$$K_e = M_{fd} \cdot I_f = 1.07 \times 1.32 = 1.41 \text{ V/rd/s}.$$

4.4 Determination of the static torque C_s and the friction coefficient K_f

For a DC motor with separate excitation, the electromagnetic torque is expressed by the relationship:

$$C_{em} = 1.41 \cdot I_a. \tag{20}$$

We keep the excitation current of the motor constant and equal to its nominal value then the expression of the torque becomes:

$$C_{em} = K_e \cdot I_a \text{ with } K_e = M_{fd} \cdot I_f. \tag{21}$$

The armature voltage is varied. Afterwards, the different values of the armature current and the speed of the rotor are recorded by a tachometer for each voltage.

The characteristic $C_{em}(\omega_r)$ is then plotted. The electromagnetic torque can be measured by a torque meter or calculated by the relationship $C_{em} = M_{fd} \cdot I_f \cdot I_a$ after measuring the armature current, as shown in Fig. 9. The obtained results are represented by Table 7. From Table 7, we can draw the graph of the couple according to the speed given by Fig. 10.

The extension of the characteristic $C_{em}(\omega_r)$ at the origin intersects the ordinate axis at a point. The latter designates the value of the static torque $C_s = 1.51$ Nm. The slope of the $C_{em}(\omega_r)$ represents the friction coefficient $K_f = 0.0045$ Nm/rd/s.

4.5 Determination of the inertia of rotating masses

The motor is wired as separate excitation. The field current is fixed at its nominal value and the motor is started by gradually increasing its armature voltage. The speed is fixed at its nominal value (1500 rpm), using a memory oscilloscope, the curve of the decrease in the rotational speed of the motor is recorded as a function of time $\omega_r(t)$, as shown in Fig. 11.
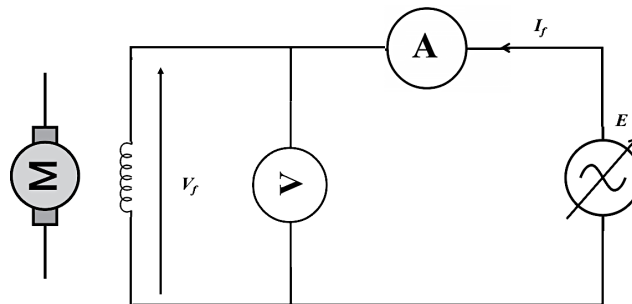
Fig. 7 Determination of the e.m.f. constant K_e

Table 6 Results obtained to determine the constant K_e

Measured I_f (A)	0.12	0.25	0.375	0.5	0.75	0.9	1.025	1.17	1.36	1.46	1.56	1.67	1.8	1.88
Measured V_a (V)	21	42	61	84	126	153	171	192	213	222	231	237	243	245
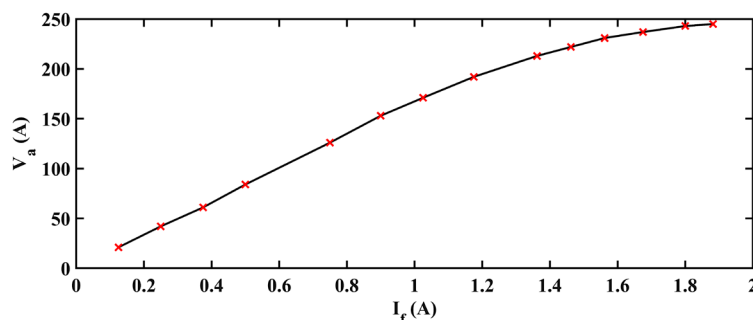
Fig. 8 $V_a(I_f)$ curve
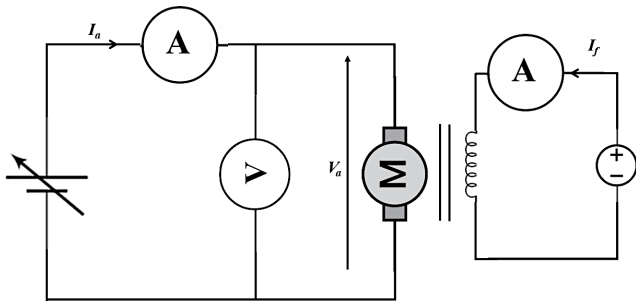
Fig. 9 Determination of the static torque C_s and the friction coefficient K_f

Table 7 The obtained results to determine C_s and K_f

V_a (V)	49	101	154	189	204	216	224
I_a (A)	1.3	1.4	1.51	1.52	1.53	1.6	1.65
ω_r(rd/s)	33.0	70.3	108.7	134.0	144.9	153.5	158.9
C_{em}(Nm)	1.69	1.9	2.05	2.13	2.16	2.26	2.33
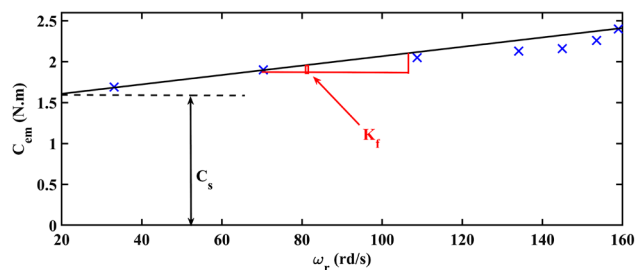
Fig. 10 The curve of $C_{em}(\omega_r)$
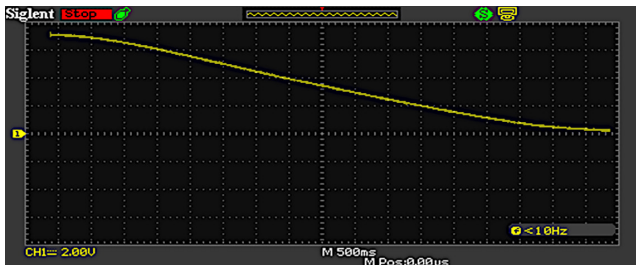
Fig. 11 Rate of speed as a function of time during deceleration

From the deceleration curve recorded by the oscilloscope, we can derive the deceleration time T_r (T_r=8 s). We can deduce the value of the inertia J by the following relation:

$$J = K_f \cdot T = 0.0045 \cdot 8 = 0.036 \text{ Kg} \cdot \text{m}^2.$$

5 DC motor speed regulation

The structure of a speed regulator generally comprises two cascaded regulation loops, The main variable to be controlled is the speed. To achieve this regulator, the voltage corresponding to the real speed of the motor must be compared with the speed reference voltage. The second loop controls the armature current, as shown in Fig. 12.

5.1 Sizing of the controllers' parameters

In order to regulate the speed of our motor, we have chosen two PI regulators; one for the speed loop and another for the current loop.

5.1.1 Structure of a PI regulator

The general structure of a proportional integral regulator shown by the Fig. 13 is composed of the proportional function and the integral function placed in parallel. Its transfer function is given by:

$$R(p) = K_1 + \frac{K_2}{P} = \frac{K_1 P + K_2}{P} = K\left(1 + \frac{1}{T_i P}\right), \quad (22)$$

with $K = K_1$ and $T_i = K_1 / K_2$.

The main advantage of a PI regulator is that it cancels the static error thanks to the integral function. Indeed, it calculates the command $u(t)$ to be injected into the system by integrating the error magnitude $e(t)$. Thus, the command signal increases as long as the error signal is non-zero, the
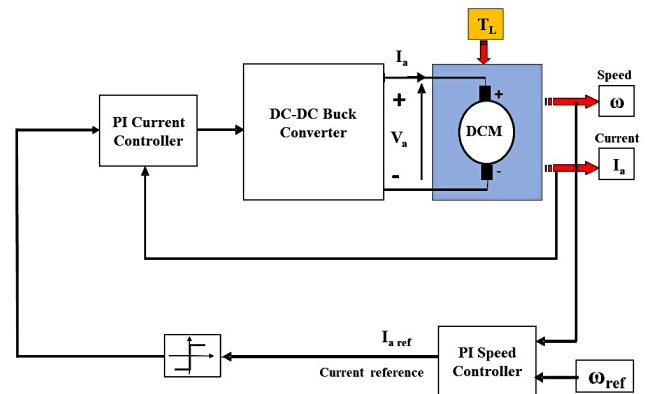
Fig. 12 Principle of speed regulation of a DC motor

Fig. 13 Structure of the PI regulator

command $u(t)$ does not stop growing as long as the error between the output $y(t)$ and the reference $y_{ref}(t)$ is not nil.

The closed loop transfer function is given by:

$$G_{CL}(p) = \frac{K_1 \left(P + \dfrac{K_2}{K_1} \right) G(P)}{1 + K_1 \left(P + \dfrac{K_2}{K_1} \right) G(P)}, \tag{23}$$

which shows that the PI regulator adds a zero to the closed loop transfer function. This can optionally be used to compensate for a pole of the transfer function of the system, thus simplifying the order of the closed-loop transfer.

5.1.2 The pole compensation method

This method takes place in two stages, it consists, in a first stage, in using the zero of the regulator to compensate the pole of the system [22]. It thus makes it possible to simplify the order of the transfer function in open loop. This compensation gives the first equation making it possible to calculate the two parameters K_1 and K_2. In a second step, the closed-loop transfer function is calculated, and a second equation is determined allowing the second coefficient of the regulator to be calculated.

5.2 Calculation of regulators parameters

Fig. 14 represents the Matlab Simulink diagram which includes the global regulation system.

In order to calculate the parameters of the regulators we have opted for the pole compensation method.

5.2.1 Calculation of the current regulator parameters

Current overshoots are a real problem, both for the static converter and for the motor, current transients risk destroying the power components of the static converter. In addition, the motor conductors' risk being destroyed by overcurrent. For these reasons it is therefore necessary:

- control the current to control overtaking;
- to limit the maximum current to protect the motor in all cases.

The calculation of the parameters of the DC motor current regulator is done from the block diagram shown in the following Fig. 15.

We have:

$$G_i(p) = \frac{I_a(p)}{V_e(p)}, \tag{24}$$

$$I_a(p) = \frac{1}{R_a + L_a \cdot P} V_a(p), \tag{25}$$

$$I_a(p) = \frac{1}{R_a + L_a \cdot P} \frac{K_{cm}}{1 + T_{cm} \cdot P} V_e(p), \tag{26}$$

then:

$$G_i(p) = \frac{K_{cm}}{(1 + T_{cm} \cdot P)(R_a + L_a \cdot P)}. \tag{27}$$

We know that $T_e = L_a / R_a$:

$$G_i(p) = \frac{K_{cm} / R_a}{(1 + T_{cm})(1 + T_e \cdot P)}, \tag{28}$$
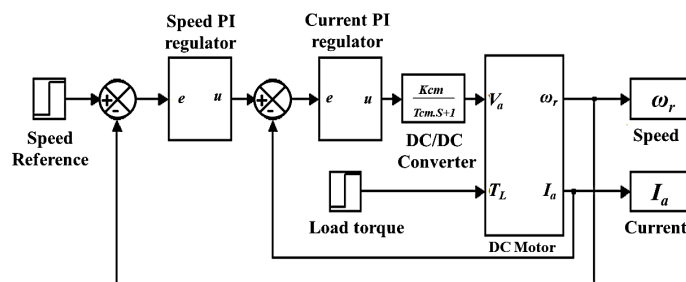
Fig. 14 Matlab Simulink bloc of the global system
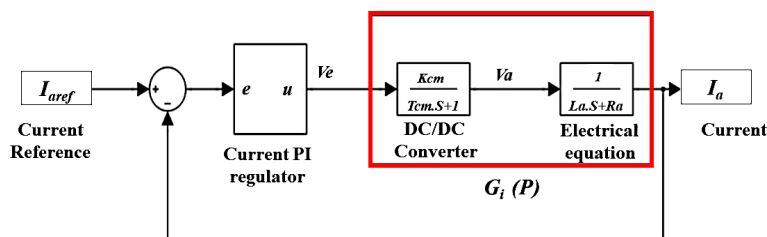
Fig. 15 Simulink bloc of the current loop

and $T_{cm} \ll T_e$ we get:

$$G_i(p) = \frac{K_{cm}/R_a}{(1+T_e \cdot P)} = \frac{G_{0i}}{(1+T_e \cdot P)}. \tag{29}$$

The transfer function being that of a first order, so the solution is a simple PI correction:

$$R_i(p) = K_{pi} + \frac{K_{ii}}{P}, \tag{30}$$

which is equal to:

$$R_i(p) = \frac{P \cdot K_{pi} + K_{ii}}{P} = \left(\frac{P\frac{K_{pi}}{K_{ii}}+1}{P} \right) K_{ii} = K_{ii} \frac{(1+T_i P)}{P}. \tag{31}$$

The simplest choice then consists in compensating the electric pole by choosing $K_{pi}/K_{ii} = T_i = T_e$ which leads to a closed loop system of a transfer function of order 1 as shown in the Fig. 16.

The transfer function G_{iCL} of the global system is given by:

$$G_{iCL}(p) = \frac{C_i(p) \cdot G_i(p)}{1 + C_i(p) \cdot G_i(p)}, \tag{32}$$

$$G_{iCL}(p) = \frac{K_{ii}\frac{(1+T_i P)}{P}\frac{G_{0i}}{(1+T_e \cdot P)}}{1 + K_{ii}\frac{(1+T_i P)}{P}\frac{G_{0i}}{(1+T_e \cdot P)}}. \tag{33}$$

After the compensation of the electric pole:

$$G_{iCL}(p) = \frac{K_{ii} \cdot G_{0i}}{P + K_{ii} \cdot G_{0i}} = \frac{1}{1+\frac{1}{K_{ii} \cdot G_{0i}}P} = \frac{1}{1+T_{bf} \cdot P}. \tag{34}$$

We deduce by identification

$$T_{bf} = \frac{1}{K_{ii}G_{0i}} = T_e, \tag{35}$$

from were:

$$K_{ii} = \frac{1}{G_{0i}T_e}, \tag{36}$$

$$K_{pi} = T_e \cdot K_{ii}. \tag{37}$$

5.2.2 Calculation of the speed regulator parameters
Once the current loop is set, you can easily set the speed loop (Fig. 17). The calculation of the parameters of the DC motor speed regulator is done from the following block diagram.

Considering that the current I_a is exactly I_{aref}, the speed transfer function is therefore:

$$G_{\omega r}(p) = \frac{\omega_r(p)}{I_{aref}(p)}. \tag{38}$$

This function is of order 4. The calculation of the parameters of the speed regulator in this case will be difficult. In order to avoid this difficulty, we will proceed as follows.

It suffices to send a step of amplitude 1 to the system, the response obtained is similar to that of the first order system, whose transfer function is given by:
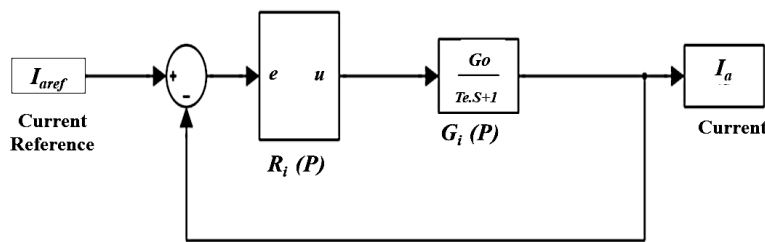
Fig. 16 Simulink bloc of the current closed loop
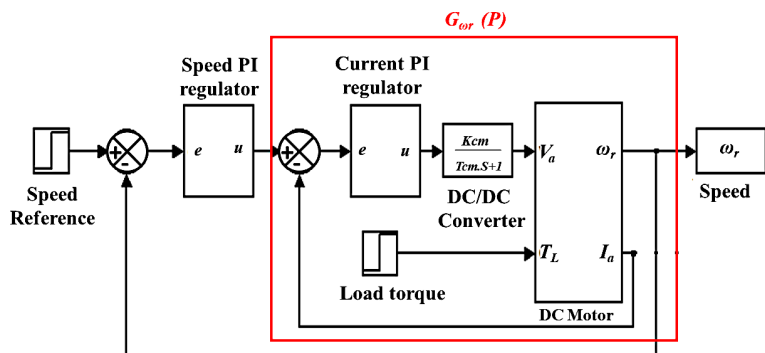
Fig. 17 Simulink bloc of the speed closed loop

$$G_{\omega r}(p) = \frac{G_{0\omega}}{1 + T_{\omega} \cdot P}. \tag{39}$$

The response of the system is represented by the following curve Fig. 18.

Now we can easily deduce the parameters ($G_{o\omega}$ and T_{ω}) of the transfer function of the system. The gain $G_{o\omega} = 313.33$ dB represents the final value of ω_r and the time constant $T_{\omega} = 9.38$ s corresponds to 63% of the final value of ω_r.

We note that the response time is important, so in order to get a faster response, we can take the time constant of the motor alone. So we supply the motor directly with its nominal voltage, then we draw the time constant through the speed curve.

We can derive the new value of the closed loop time constant of the speed which is:

$$T_{bf\omega} = 0.025 \text{ s.}$$

We can now obtain the parameters of the speed transfer function as follow:

$$G_{\omega r}(p) = \frac{313.33}{1 + 0.025 \cdot P}. \tag{40}$$

After the calculation we find the speed regulator parameters:

$$K_{i\omega} = \frac{1}{G_{0\omega} \cdot T_{bf\omega}}, \tag{41}$$

$$K_{p\omega} = T_{\omega} \cdot K_{i\omega}. \tag{42}$$

5.3 Simulation results

The controller was simulated using Matlab-Simulink software. Two performance testing are made as follow:

1. Test 1: The reference speed is set at the nominal value $\omega_{ref} = 157$ rad/s and the load torque changes according to the protocol shown in Fig. 19. The results of the simulation are shown in Figs. 20 and 21.
2. Test 2: The reference speed change with the load conditions (5 Nm), the results of the simulation are shown in Figs. 22 and 23.

The first test shows the robustness of the control with respect to the load variation. The rapidity of the motor speed response illustrates the good performance of the control law.

From the results of the second test; despite the sudden change in the speed set point, the applied control responds perfectly to this disturbance. It can be observed that the motor speed converges rapidly to its reference, and it is well maintained at this value. As for the armature current, it follows its reference perfectly.

The obtained results confirm that the proposed control scheme and the calculated parameters give a good result. It is clear that the proposed PI controllers permit to regulate the motor speed to its reference in a short time. This controller ensures a good tracking of the armature current in a short time and is perfectly maintained between the desired bands.
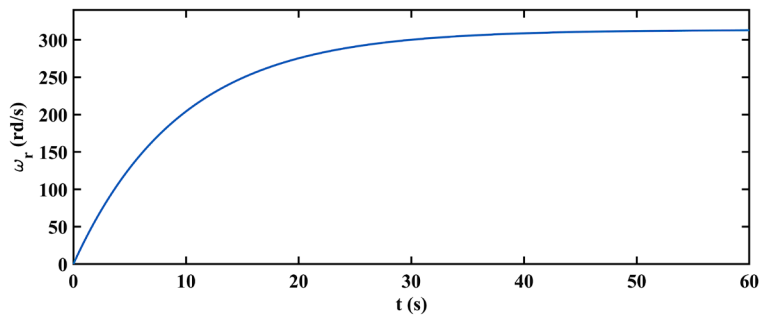
Fig. 18 System response
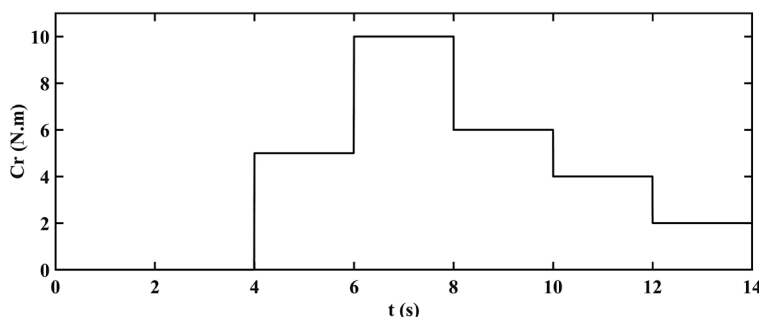
Fig. 19 Protocol of the torque
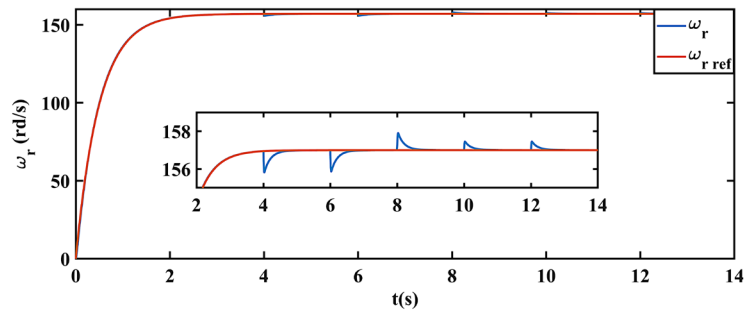
(a)
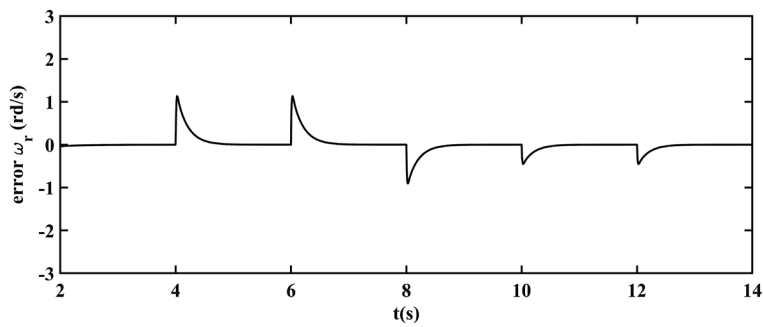
(b)

Fig. 20 Torque variation test; (a) ω_r, $\omega_{r\,ref}$; (b) $\omega_{r\,ref} - \omega_r$
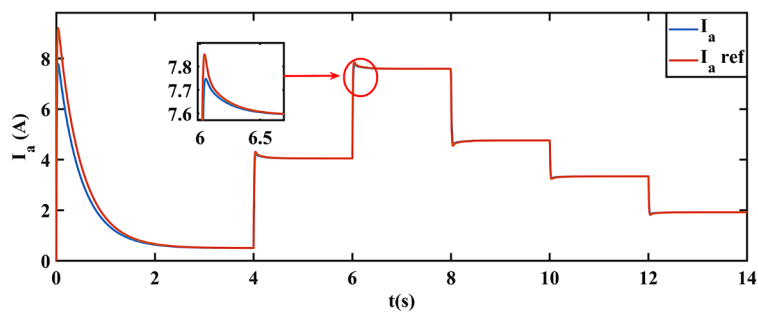
(a)
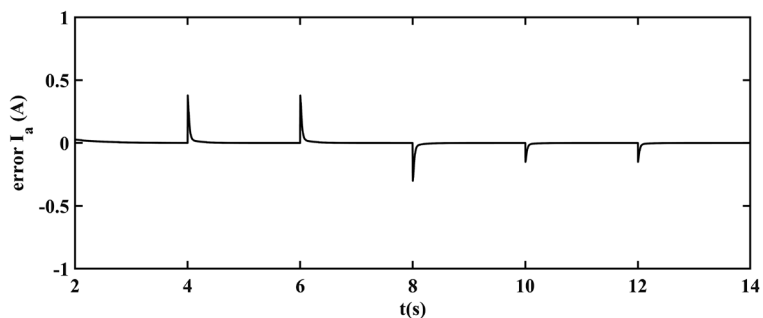
(b)

Fig. 21 Torque variation test; (a) I_a, $I_{a\,ref}$; (b) $I_{a\,ref} - I_a$

6 Description of the test bench

To validate experimentally the control technique presented in this work, we have built a test bench. The latter consists of a converter (series chopper), whose arm switches consist of an IGBT transistor mounted in antiparallel with a diode, the IGBT control signal comes from a Dspace1103 card
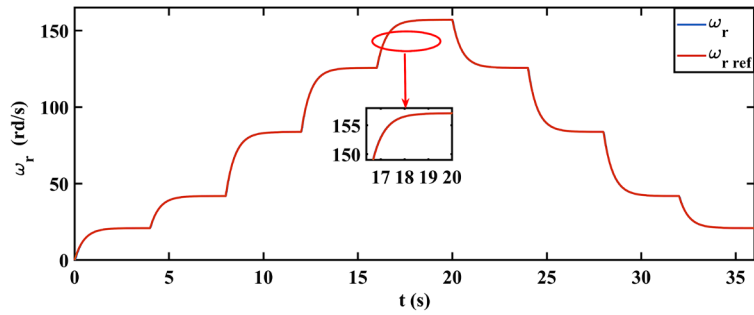
Fig. 22 Speed reference variation test (ω_r, $\omega_{r\,ref}$)
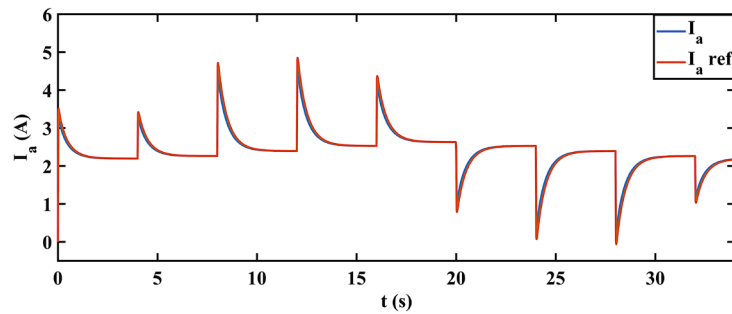
Fig. 23 Speed reference variation test (I_a, $I_{a\,ref}$)

based on a processor dedicated to signal processing. The photography of this experimental bench is shown in Fig. 24.

This test bench highlights three different parts:

1. The power part which includes the converter (series chopper), and the load, consisting of a DC motor. The power switches employed in the realized chopper are composed of an IGBT module and a diode, where the reference is SKM 120 GB 123 from Semikron.

These modules support a voltage of 600V and allow the passage of a current of 120A.

2. The measurement part, made up of current sensor (to measure the armature current) and a speed sensor to measure the motor speed. The current is measured using a Hall effect current sensor (LEM LA-55 P). This sensor has a bandwidth of 200 KHz and a transformation ratio of 1/1000.
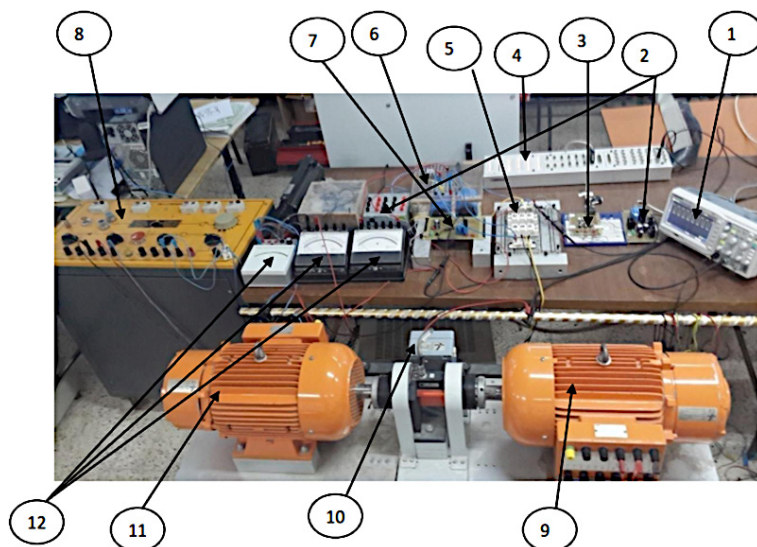
Fig. 24 Experimental bench; 1: Digital oscilloscope; 2: Symmetric power supply; 3: Command card; 4: Dspace1103 control panel; 5: IGBT module; 6: Filtering capacitor; 7: Current sensor; 8: Control desk; 9: Asynchronous machine; 10: Speed sensor; 11: Direct current machine; 12: Ammeters and voltmeters

3. The control part consists of a Dspace1103 control card (based on a TMS320F240 DSP) controlled by a computer. The computer is used to generate the defined object code from the control algorithm.

The ControlDesk software, which is associated with the Dspace, allows to follow the execution of the program implemented in the DSP, by displaying the evolution curves of the variables, and by offering the possibility to modify these variables in real time [23].

The arm has a single control board that generates a two-state signal. The board is powered by a symmetrical source which delivers a voltage of 5V to power the Optocouplers and 15V to power the Drivers.

The IGBT is driven by an igniter (Driver) which allows to adapt the control signals to the characteristics of the switches. The driver IR2109 is an integrated circuit used to improve the switching times of power electronics switches. The output of the driver sends a variable DC voltage of 0–15 V across the switches of the module.

In order to ensure an isolation between the control board and the power part, the 4N35 Optocoupler is used. Where the outputs are connected to the driver, this isolation allows us to protect the low power electronic part and to allow it to be less sensitive to the noise generated by the power part.

6.1 Experimental results

According to the Fig. 25, the sensed speed of the motor follows the reference speed imposed at the start with spikes which are due to the current spikes absorbed by the motor when passing from one speed level to another. We also notice the speed captured, has ripples which are due to the regulation which has some overruns and also to the different materials used which have certain measurement errors. Beyond that, the motor starts and operates at the desired speed without posing the slightest risk to the control part.

We see that the current picked up follows the reference (Fig. 26), but it has peaks due to the passage of the motor from one speed to another.

We also note that the current represents some ripples imposed by the instants of switching of the control switch, otherwise the current loop operates without posing any risk to the control part.

7 Conclusion

Our objective was the identification of the parameters of an independently excited DC machine and then to design and implement a speed control of this machine using the Dspace1103 board. Tests were carried out on the DCM in order to identify its parameters; the simulation and experimental results show a normal behavior of the machine,
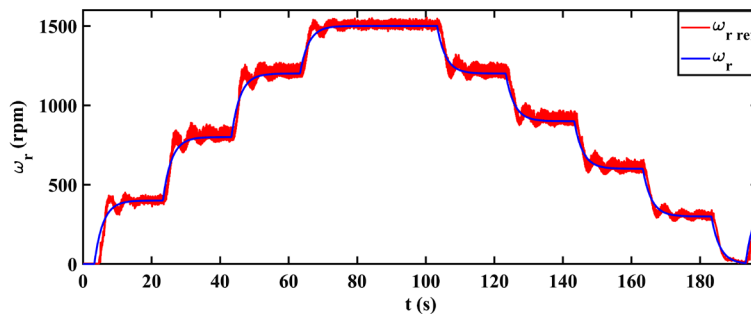
Fig. 25 Motor speed and its reference
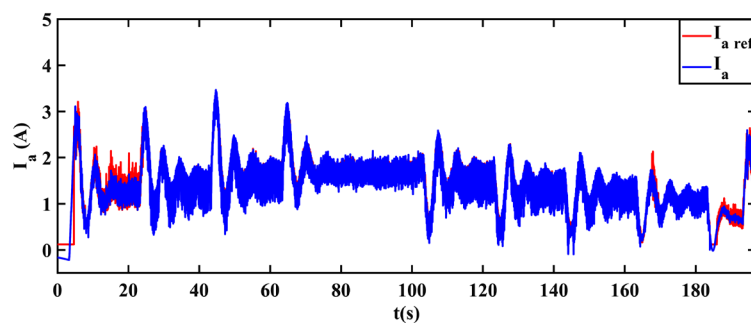
Fig. 26 Armature current and its reference

which confirms that the identified parameters are very close to the real parameters of the machine. Using the ControlDesk software interface that is associated with the Dspace1103 and Matlab simulink, we implemented the control algorithm that allows the sending of a PWM signal to control a serial chopper. This converter consists in varying the speed of a separately excited DC machine by varying the armature voltage. The results obtained show that the regulated current and speed practically follow their references with some overshoots and ripples, due to the lack of precision of the equipment available in the laboratory. We can confirm that the objective, set at the beginning, has been achieved and our work meets the requirements determined at the beginning.

References

[1] Sands, T. "Control of DC Motors to Guide Unmanned Underwater Vehicles", Applied Sciences, 11(5), 2144, 2021.
https://doi.org/10.3390/app11052144

[2] Izci, D., Ekinci, S. "An Efficient FOPID Controller Design for Vehicle Cruise Control System Using HHO Algorithm", In: 2021 3rd International Congress on Human-Computer Interaction, Optimization and Robotic Applications, Ankara, Turkey, 2021, pp. 1–5. ISBN 978-1-6654-1165-3
https://doi.org/10.1109/HORA52670.2021.9461336

[3] Izci, D., Ekinci, S. "A Novel Hybrid ASO-NM Algorithm and Its Application to Automobile Cruise Control System", In: Proceedings of 2nd International Conference on Artificial Intelligence: Advances and Applications, Jaipur, India, 2022, pp. 333–343. ISBN 978-981-16-6332-1
https://doi.org/10.1007/978-981-16-6332-1_29

[4] Hari Priya, U., Jyothi, P., Phanipavan, V. V. S. S., Deepa, K., Jain, A. "Energy Conservation Strategy for DC Motor Load Applications", In: Balas, V. E., Kumar, R., Srivastava, R. (eds.) Recent Trends and Advances in Artificial Intelligence and Internet of Things, Springer Cham, 2020, pp. 177–186. ISBN 978-3-030-32644-9
https://doi.org/10.1007/978-3-030-32644-9_19

[5] Khalifa, M., Amhedb, A. L. H., Al Sharqawi, M. "Position Control of Real Time DC Motor Using LabVIEW", Journal of Robotics and Control (JRC), 2(5), pp. 342–348, 2021.
https://doi.org/10.18196/jrc.25104

[6] Mahmood, Z. S., Nasret, A. N., Mahmood, O. T. "Separately excited DC motor speed using ANN neural network", AIP Conference Proceedings, 2404, 080012, 2021.
https://doi.org/10.1063/5.0068893

[7] Pinto, V. H., Gonçalves, J., Costa, P. "Model of a DC Motor with Worm Gearbox", In: APCA International Conference on Automatic Control and Soft Computing, Bragança, Portugal, 2020, pp. 638–647. ISBN 978-3-030-58652-2
https://doi.org/10.1007/978-3-030-58653-9_61

[8] Becedas, J., Mamani, G., Feliu, V. "Algebraic parameters identification of DC motors: methodology and analysis", International Journal of Systems Science, 41(10), pp. 1241–1255, 2010.
https://doi.org/10.1080/00207720903244097

[9] Saab, S. S., Kaed-Bey, R. A. "Parameter identification of a DC motor: an experimental approach", In: ICECS 2001. 8th IEEE International Conference on Electronics, Circuits and Systems (Cat. No.01EX483), Malta, Malta, 2001, pp. 981–984.
https://doi.org/10.1109/ICECS.2001.957638

[10] Hamida, M. L., Denoun, H., Fekik, A., Vaidyanathan, S. "Control of separately excited DC motor with series multi-cells chopper using PI - Petri nets controller", Nonlinear Engineering, 8(1), pp. 32–38, 2019.
https://doi.org/10.1515/nleng-2017-0174

[11] Volosencu, C. "Reducing Energy Consumption and Increasing the Performances of AC Motor Drives Using Fuzzy PI Speed Controllers", Energies, 14(8), 2083, 2021.
https://doi.org/10.3390/en14082083

[12] Voloşencu, C. "Stability Analysis of Systems with Fuzzy PI Controllers Applied to Electric Drives", Mathematics, 9(11), 1246, 2021.
https://doi.org/10.3390/math9111246

[13] Shin, H. B. "New antiwindup PI controller for variable-speed motor drives", IEEE Transactions on Industrial Electronics, 45(3), pp. 445–450, 1998.
https://doi.org/10.1109/41.679002

[14] Desoer, C., Lin, C. A. "Tracking and disturbance rejection of MIMO nonlinear systems with PI controller", IEEE Transactions on Automatic Control, 30(9), pp. 861–867, 1985.
https://doi.org/10.1109/TAC.1985.1104078

[15] O'Dwyer, A. "A Summary of PI and PID Controller Tuning Rules for Processes with Time Delay. Part 1: PI Controller Tuning Rules", IFAC Proceedings Volumes, 33(4), pp. 159–164, 2000.
https://doi.org/10.1016/S1474-6670(17)38237-X

[16] Harrouz, A., Becheri, H., Colak, I., Kayisli, K. "Backstepping control of a separately excited DC motor", Electrical Engineering, 100(3), pp. 1393–1403, 2018.
https://doi.org/10.1007/s00202-017-0592-5

[17] Arof, S., Ahmad, M. R., Mawby, P., Arof, H., Noorsal, E. "Comparative Study on the Performance of Electrical Vehicles with DC Drive and Series Motor, DC Drive and Separately Excited DC Motor, and AC Drive and PMSM Motor. Part 1: Driving and Braking Operations", In: Bakar, M. H. A., Razak, M. A. H. A., Öchsner, A. (eds.) Progress in Engineering Technology IV, Springer Cham, 2020, pp. 121-138. ISBN 978-3-030-93250-3
https://doi.org/10.1007/978-3-030-93250-3_11

[18] Avitan, I., Skormin, V. "Mathematical modeling and computer simulation of a separately excited DC motor with independent armature/field control", IEEE Transactions on Industrial Electronics, 37(6), pp. 483–489, 1990.
https://doi.org/10.1109/41.103452

[19] Virgala, I., Kelemen, M. "Experimental Friction Identification of a DC Motor", International Journal of Mechanics and Applications, 3(1), pp. 26–30, 2013.
https://doi.org/10.5923/j.mechanics.20130301.04

[20] Hadef, M., Mekideche, M. R. "Parameter identification of a separately excited dc motor via inverse problem methodology", Turkish Journal of Electrical Engineering & Computer Sciences, 17(2), pp. 99–106, 2009.
https://doi.org/10.3906/elk-0805-5

[21] Abdessemed, R., Kadjouj, M. "Modélisation des machines électriques" (Modeling of electrical machines), Presse de l'université de Batna, Batna, Algeria, 1997. (in French)

[22] Derbel, H. B. J. "Design of PID controllers for time-delay systems by the pole compensation technique", In: 2009 6th International Multi-Conference on Systems, Signals and Devices, Djerba, Tunisia, 2009, pp. 1–6. ISBN 978-1-4244-4345-1
https://doi.org/10.1109/SSD.2009.4956670

[23] Darkawi, A. "Initiation au système dSPACE, de l'interface RTI dans Simulink et de ControlDesk Next Generation 5.4 version 2.0" (Introduction to dSPACE system, RTI interface in Simulink and ControlDesk Next Generation 5.4 version 2.0), [computer program] Available at: https://hal.archives-ouvertes.fr/cel-01259564 [Accessed: 06 May 2022] (in French)